Indian Journal of Chemical Technology
Vol. 25, July 2018, pp. 376-382

Fast and efficient removal of Acid Brown 214 from aqueous media by adsorption onto fluorene functionalized nanoporous SBA-15

Shiva Dehghan Abkenar
Department of Chemistry, Savadkooh Branch,
Islamic Azad University, Savadkooh, Iran
E-mail: dehghan54@yahoo.com

Received 30 September 2016; accepted 13 February 2017

Fluorene functionalized nanoporous SBA-15 has been used as a novel solid phase adsorbent for removal of acid brown 214 from water solution. SBA-15 grafted with N-(4-(trimethylsilyl)butyl)-9*H*-fluorene-9-amine has been synthesized according to procedure in the literature. Structural properties of the prepared materials have been characterized by FT-IR, Raman spectrum, TGA, and XRD analyses and nitrogen physisorption isotherms. Dye removal using adsorption requires a proper study to determine its optimal performance characteristics. In this study, the effects of *p*H, the amount of adsorbent, contact time and dye concentration on adsorption were determined in order to find the optimum adsorption conditions. The data fits well to the Langmuir model with maximum adsorption capacities 454.5 mg/g for Acid Brown 214 under *p*H=4. Also the adsorption kinetics parameters have been studied and evaluated. Adsorption of acid brown 214 on fluorene functionalized nanoporous SBA-15 reached equilibrium after 5 min and follows the pseudo-second order kinetic model. Desorption process of the adsorbed dye is also investigated.

Keywords: Dye removal, Acid Brown 214, N-(4-(trimethylsilyl) butyl)-9*H*-fluorene-9-amine functionalized SBA-15

Synthetic organic dyes are one of the major pollutants and water contaminants in effluents of textile, leather, paper, plastic, printing, food, and mineral processing industries[1–3]. Aromatic dyes, especially azo dyes, cause severe ecological problems and are classified as environmentally hazardous materials due to their toxicity and slow degradation[4–6]. Treatment of industrial effluents containing carcinogenic and mutagenic azo dyes is necessary prior to their final discharge to the environment and meets the stringent environmental regulations[7–10].

Azo dyes are highly soluble in water and their removal from wastewater is difficult by conventional coagulation and activated sludge processes[11]. These dyes are not normally removed by conventional wastewater treatment systems. Therefore, the employment of these dyes must be controlled, and the effluents must be treated before being released into the aquatic and terrestrial environment[12,13]. Hence, it becomes imperative that azo dyes are removed from the effluents before it is disposed off.

Currently, several physical or chemical processes are used to treat dye-laden wastewaters, such as adsorption[14-18], and chemical oxidation[10,19], electro-chemical oxidation [20], and photocatalytic oxidation[21], Adsorption techniques are quite popular due to their simplicity and highly effective methods for removal of dye from wastewater [22] and the adsorbent was frequently used in the treating processes. The adsorbent for removal of dyestuffs from wastewater includes activated carbon, magnetic nanoparticles, zeolite, montmorillonite and other natural materials[23-27]. The ideal adsorbent should have a stable and accessible pore structure with uniform pore size distribution as well as high surface area. Mesoporous materials exhibit a number of potential advantages as adsorbents for the removal of dyes from waste water[28-30]. The development of functionalized mesoporous materials for adsorption applications including the removal of dyes has generated a considerable interest. For adsorption processes, a variety of functional groups can be grafted or incorporated on the surface of mesoporous channels and prepare highly effective adsorbents[31,32]. Mesoporous materials, such as SBA-3[33], ammonium functionalized MCM-41[34], and silane-modified HMS[35], have been found to be as suitable adsorbents for the removal of dyes from wastewater.

The study of mesoporous silica molecular sieves has attained considerable attention due to their high surface area, large pore volume, and good performance as effective adsorbents. The discovery of SBA-15 is a significant progress in the field of mesoporous materials. The hexagonally arranged and highly ordered SBA-15 materials possess many advantages such as easy synthesis, tunable pore size, and thick pore wall[36]. The specific porous structure and the excellent textual properties allow easier diffusion of target molecules into the active sites. Therefore, they have been used for various applications and shown to be of considerable performance.

In this study SBA-15 grafted with N-(4-(trimethylsilyl) butyl)-9*H*-fluorene-9-amine (fluorene functionalized SBA-15) has been prepared and characterized and then these prepared materials were applied as a new adsorbent to remove of typical triazo acid dye, Acid Brown 214 (AB 214). The applicability of this adsorbent has been evaluated in view of the effects of solution *p*H, adsorbent dosage, dye concentration and contact time. To the best of our knowledge, there is no previous report on adsorption techniques to removal of acid brown 214 from aqueous media.

Experimental Section

The *p*H was controlled by Metrohm *p*H-meter model 713 and Shimadzoλ 25 double beam spectrophotometer was used for the detection of dye concentration in the solution.

FT-IR spectra were obtained on Equinox 55 spectrometer. Raman spectra were obtained on SENTERRA spectrometer. Small and wide angle X-ray scattering (XRD) patterns were recorded with a model Hecus S3-MICROpix SAXS diffractometer with a one-dimensional PSD detector using Cu Kα radation (50KV, 1mA) at wave length 1.542 A°. Thermogravimetric analysis (TGA) was performed on a TA Q50 instrument. The scans were performed between 25 and 800°C at 10°C/min. Elemental analyses was carried out by a Rapid elemental analyzer. Nitrogen physisorption isotherms were obtained on a BELSORP mini-II at liquid nitrogen temperature (77K). Surface area was measured using the Brunnauer-Emmett-Teller (BET) method, pore size distributions were calculated from the nitrogen isotherms by Barret-Joyner-Halenda (BJH) method.

All Chemicals were of the reagent–grade and purchased from Fluka and Merck chemical companies. Double distilled water (DDW) was used throughout the study. The pipettes and vessels used for trace analysis were kept in dilute nitric acid for at least 24 hr and subsequently washed four times with DDW before use.

The stock solution of dye was prepared by dissolving dye powder in DDW and diluted to prepare the desired concentration of dye solutions.

Synthesis of fluorene functionalized nanoporous SBA-15

SBA-15 material was synthesized by following the procedure reported in literature[37-40]. Aminopropyl functionlized SBA-15 material was synthesized by following the procedure reported by Zheo *et al.* [40]. Aminopropyl functionlized SBA-15 (2 g) was placed under vacuum for 30 min, then 80 mL dry toluene was added and stirred for 15 min, 9-bromofluorene[41] (1.11 g, 4.5 mmol) was added to the resulting mixture under inert atmosphere (Ar) and reflux for 24 hr. Then it was cooled at room temperature and toluene was removed by filtration under vacuum. It was dried at room temperature and functionalized silica was washed with ethanol by using a soxhlet apparatus for 3 days, followed by drying at room temperature to remove ethanol. The structural formula is given in Fig. 1.

Dyes removal experiment

Batch adsorption experiments were conducted with the fluorene functionalized nanoporous silica SBA-15 for the removal of AB 214 from aqueous solutions. Equilibrium adsorption experiments were conducted by adding 0.010 g of fluorene functionalized nanoporous silica into 10 mL of 50 mgL^{-1} of each of acidic dye solution at *p*H 4. All of the adsorption experiments were conducted in triplicate. The mixed solution was gently shacked at room temperature for 5 min. At the end of the adsorption period, the supernatant was centrifuged for 5 min at 3800 rpm. The residual amounts of dyes in the solution were determined spectrophotometrically at 486 nm for AB 214.

The adsorption percentage for dye, i.e. the dye removal efficiency, was determined using the following expression:

$$\% R = \left[\frac{(C_o - C_t}{C_o}\right] \times 100$$

C_o and C_t represent the initial and final (after adsorption) concentration of dye (mgL^{-1}), respectively.

All the experiments were performed at room temperature. The effects of *p*H, the amount of adsorbent, contact time and dye concentration on adsorption were investigated. The adsorption kinetic was determined by analyzing adsorption capacity of the aqueous solution at different time interval. For adsorption isotherm, the dye solution of different concentration in the range of 50-1000 mgL^{-1} was agitated until the equilibrium was achieved. The

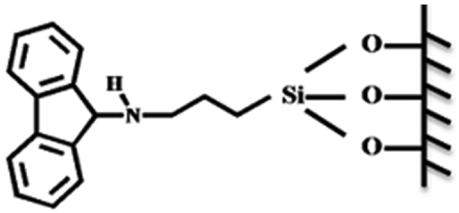

Fig. 1 — The structure of fluorene functionalized SBA-15

adsorbed amounts (q_e) of dye were calculated by the following equation:

$$q_e = \left[\frac{C_o - C_e}{m}\right] \times V$$

where C_o and C_e are the initial and equilibrium concentrations of dye in mgL^{-1}, m is the mass of adsorbent (g), and V is the volume of solution (L).

Results and Discussion

Adsorbent characterization

Figure 2a shows the small angle XRD patterns of the fluorene functionalized SBA-15. The sample have a single intensive reflection at 2θ angle around 0.87° similar to the typical SBA-15 materials, that is generally recognized to the long-range periodic[40]. Also two additional peaks related to the higher ordering (110) and (200) reflections are also observed, which is associated with a two-dimensional hexagonal (p6mm) structure[41]. However, in the case of functionalized SBA-15 material, the peak (100) intensity decreases after immobilizations due to the difference in the scattering difference of the pores and the walls, and to the irregular covering of organic groups on the nanochannels[36].

The textural properties of the sample were evaluated by the nitrogen adsorption-desorption isotherm (Fig. 2b). The material exhibits a typical irreversible type IV nitrogen adsorption isotherm with an H1 hysteresis loop as defined by IUPAC[42]. The nitrogen adsorption at low relative pressures is accounted for by monolayer adsorption of N_2 on the pore walls, and does not essentially involve the presence of micropores. The sharp inflection in the P/P0 range from 0.40 to 0.60 of the isotherm is characterized as capillary condensation within uniform mesopores, the position of which is clearly correlated to a diameter in the mesopore rang. The pore size distribution can be calculated from BJH method based on the desorption branch of the N_2 adsorption isotherm. As demonstrated in Fig. 2b, a typical BJH plot from modified SBA-15 with fluorene a narrow pore size distribution is observed[43]. The uniformity of the mesopores in this modified SBA-15 is comparable to the SBA-15, indicating that the integrity of the original inorganic wall structure of the SBA-15 is retained. The textural parameters, specific surface areas (BET method), pore diameters (BJH method) and total pore volumes are given in Table 1.

Figure 2c shows FT-IR spectrum of fluorene modified SBA-15. The bands at 800 and 1086 cm^{-1}

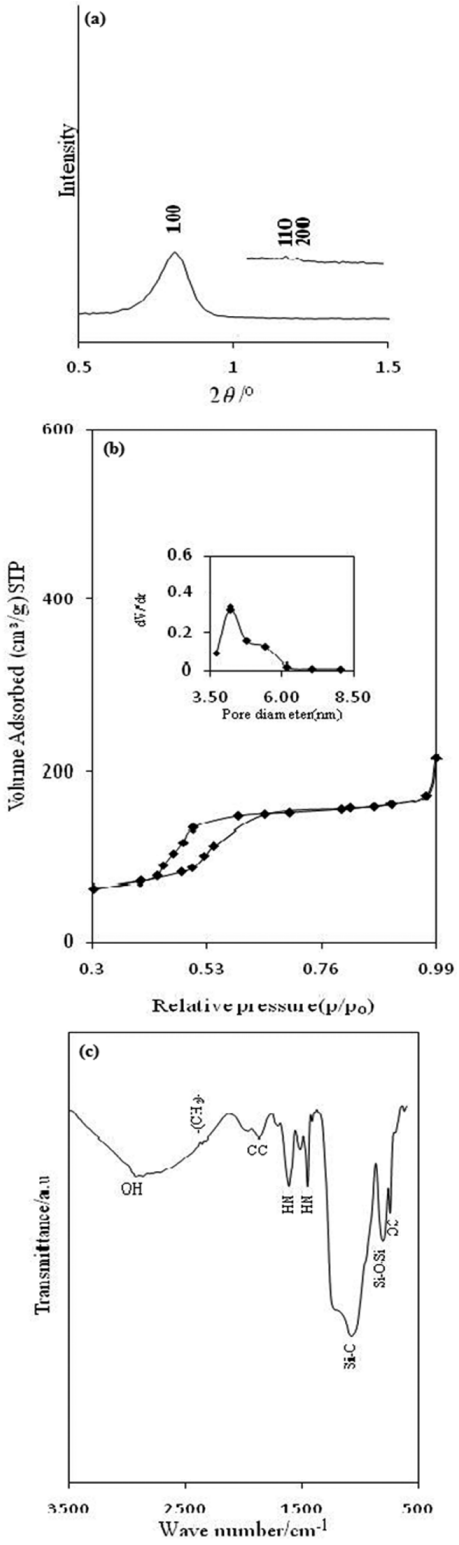

Fig. 2 — Small angle XRD pattern fluorene functionalized SBA-15 (a), Nitrogen adsorption-desorption isotherm of fluorene functionalized SBA-15, (inside: BJH pore size distribution curve of functionalized SBA-15) (b), FT-IR spectrum of fluorene functionalized SBA-15(c)

are attributed to Si-O-Si and Si-O stretching vibrations, respectively[44]. Also the adsorption bands at 1598 and 1465 cm^{-1} due to N-H bending. The band at 2930 cm^{-1} is assigned to C-H stretching vibrations of the methylene groups. The strong peak of 742 cm^{-1} was observed which due to the C=C ring skeletal vibrations and also the weak peak at 1610 and 1449 cm^{-1} are related to the same type of vibrations.

Figure 3a shows the Raman spectrum of fluorene modified SBA-15. The band at 2900 cm^{-1} is attributed to C-H stretching in the propyl chain in fluorene modified SBA-15. The strong bands at 1610, 1484 and 1024 cm^{-1} are related to the C-C and C=C ring skeletal vibrations of fluorene. The bands at 3100 and 1350 cm^{-1} are attributed to C-H ring and C-N vibrations, respectively that confirm fluorene was attached on the surface of SBA-15 (Ref.45). The IR and Raman results exhibit that fluorene is attached on the surface of SBA-15.

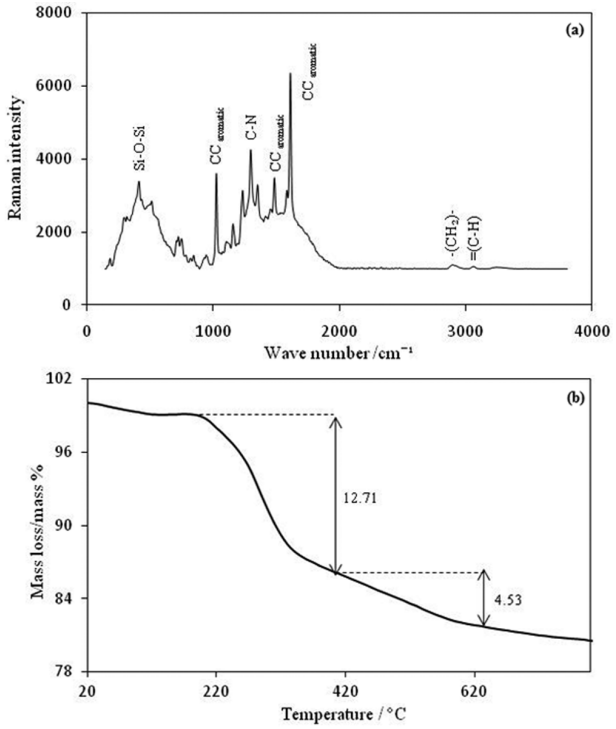

Fig. 3 — Raman spectrum (a), TGA analysis (b) of fluorene functionalized SBA-15

Table 1 — The pore diameter (D_{BJH}), BET surface area (S_{BET}) and the total pore volume (V_{total}) from nitrogen adsorption-desorption for the SBA-15 and fluorene functionalized SBA-15

Molecular sieves	D_{BJH} (nm)	S_{BET} (m^2/g)	V_{total} (cm^3/g)
SBA-15	6.2	587	0.780
Fluorene functionalized SBA-15	4.2	200	0.365

Thermogravimetric analysis (TGA) and elemental analysis were carried out to determinate the grafted amount of fluorene incorporated in SBA-15. The TGA profile sample of Y10-2 is illustrated in Fig. 3b.

The weights loss at temperature about 100°C is corresponded to the desorption of physisorbed water that is 1.5% for fluorene modified SBA-15 (Ref. 46). The weights loss (17.24 %) between 200 and 600°C are due to the decomposition of organic groups in fluorene modified SBA-15. A minor weight loss due to silanol condensation at high temperature was observed[47]. The experimental and the theoretical C/N molar ratio of fluorene modified SBA-15 was calculated from the elemental analysis data (Table 2) which confirms that fluorene is grafted to surface. The TGA is in the good agreement with the organic content determined by elemental analysis.

Effect of *p*H on the removal yield

The effect of *p*H on the adsorption of dye was stadied from *p*H 2.0 to 8.0. The *p*H was adjusted by HCl and NaOH and measured by digital *p*H meter. The *p*H may affect both aqueous chemistry and surface binding sites of the adsorbent. Acid dyes are also called anionic dyes because of they usually exist in the sulphate form. Also, at lower *p*H, the functionalized SBA-15 surface will be positively charged via protonation process, which increases the electrostatic attractions between acid dye molecules and functionalized SBA-15 surface. The adsorption of the investigated dye was increased when the *p*H of the solution increased from 2 to 4 and decrease slowly at higher *p*H values. At higher *p*H the number of positively charged sites is reduced and raised the number of negatively charged sites, creating electrostatic repulsion between the negatively charged surface of the functionalized SBA-15 and the anionic acid dyes molecules. On the other hand, the lower adsorption of acid dye, at alkaline *p*H is because of the presence of excess OH^- ions competing with the dye anions for the adsorption sites. As a result, there was in a significant reduction in the adsorption of acid

Table 2 — The elemental analysis of fluorene functionalized SBA-15

Sample	C%	N%	$C/N_{Experimental}$	$C/N_{Theoretical}$	Aminopropyl (mmol /g)	Fluorene (mmol /g)
Fluorene functionalized SBA-15	12.98	1.6	8.1	9.5	1.2	0.55

dyes from the solution. Hence, *p*H=4 was chosen for subsequence experiments.

Effect of the amount of adsorbent on removal efficiency

The effect of the amount of fluorene functionalized nanoporous silica SBA-15 as adsorbent on the removal of AB 214 was determined at room temperature and at *p*H 4.0 by varying the adsorbent amount from 0.003 to 0.020 g in 10 mL solution of 50 mg L^{-1} of dye. The results show that the removal efficiency of AB 214 was increased by increasing the amount of absorbent due to the availability of higher adsorption sites. The 0.005 g functionalized SBA-15 had a removal efficiency of 98% and then the percentage removal reached almost a constant value which is considered as complete removal of dye.

Adsorption kinetics

The equilibrium time between the pollutant and the adsorbent is of significant importance in the wastewater treatment by adsorption. For an adsorbent to be efficient in wastewater treatment, it needs to be able to show a rapid uptake of the pollutants and reach the equilibrium in a short time. Adsorption equilibrium time is determined as the time after which the concentration of the acid dye solution remains unchanged during the course of adsorption process. The effect of contact time on the amount of dye adsorbed was investigated at the initial concentration of 50 mg L^{-1} of dye at *p*H 4.0 at room temperature. The concentration of dyes was measure periodically in 3, 5, 10, 15, and 20 min. The effect of contact time on the adsorption capacity of AB 214 was studied by the functionalized nanoporous silica SBA-15. It is clear that the adsorption capacity increases rapidly during the initial adsorption stage and then continues to increase at a relatively slow speed with contact time and reaches equilibrium point after 5 min. To investigate the adsorption mechanism of AB 214 for functionalized nanoporous silica SBA-15, two kinetic models, pseudo first-order kinetic model and pseudo-second-order kinetic model, were considered to find the best fitted model for our experimental data.

The pseudo-first-order Lagergren equation is given by Lagergren:[48]

$$\log\ (q_e - q_t) = \log q_e - \frac{k_1 t}{2.303}$$

where k_1 is the pseudo-first-order rate constant (min^{-1}), q_e and q_t are amounts of dye adsorbed (mg g^{-1}) at equilibrium and at time t (min).

The pseudo-second-order model can be expressed as:

$$\frac{t}{q_t} = \frac{1}{k_2 q_e^2} + \frac{t}{q_e}$$

where, k_2 (g $mg^{-1}min^{-1}$) is the rate constant of the pseudo-second-order adsorption.[49]

Kinetic constants obtained by linear regression for the two models. The results are listed in Table 3. The correlation coefficients (R^2) for the pseudo-first-order kinetic model is relatively low and the calculated qe values ($q_{e,cal}$) from the pseudo-first-order kinetic model do not agree with the experimental data ($q_{e,exp}$), suggesting the adsorption of AB 214 onto the functionalized nanoporous silica SBA-15 cannot be applied a first order model. For the pseudo-second-order kinetic model, the R^2 value is 0.999 for AB 214 and the $q_{e,cal}$ values agreed with the $q_{e,exp}$ values very well. This indicates the applicability of the second-order model to describe the adsorption process of AB 214 onto the functionalized nanoporous silica SBA-15.

Adsorption isotherms

The equilibrium adsorption isotherm is the basic requirement in the design of adsorption systems. The adsorption capacity of AB 214 at different dye concentration in the range of 50-1000 mg/L was investigated. It is evident that the adsorption capacity of AB 214 on the functionalized nanoporous silica SBA-15 depends on the dye concentration. This may be attributed to the extent of a driving force of concentration gradients with the increase in the dye concentration. As long as there are available sites, adsorption will increase with increasing dye concentrations, but as soon as all of the sites are occupied, a further increase in concentrations of dyes does not increase the amount of dyes on adsorbents.

Two isotherm models, the Langmuir and the Freundlich models, are employed to describe the

Table 3 — Adsorption kinetic parameters of AB 214 adsorption on fluorene functionalized SBA-15

Pseudo-first order			Pseudo-second order			Experimental data
K_1 (min^{-1})	$q_{e,cal}$ (mgg^{-1})	R^2	K_2 ($gmg^{-1}min^{-1}$)	$q_{e,cal}$ (mgg^{-1})	R^2	$q_{e,exp}$ (mgg^{-1})
0.107	9.6	0. 865	26.3×10^{-3}	104.1	0.999	102.4

Table 4 — Isotherm parameters for adsorption of AB214 on fluorene functionalized SBA-15

Dye	Langmuir			Freundlich		
	q_m(mg g^{-1})	b(L mg^{-1})	R^2	K_f(mg g^{-1})	1/n	R^2
AB214	454.5	0.315	0.998	126.2	0.214	0.906

sorption behavior on fluorene functionalized nanoporous silica SBA-15 in this study. The Langmuir isotherm model[50] is based on assumptions that monolayer coverage of adsorbate occurs over homogeneous sites and a saturation point is reached where no further adsorption can act. The Freundlich isotherm model [51] is an empirical equation employed to describe heterogeneous system. Both isotherm models are represented as follows:

The linearized form of the Langmuir is:

$$C_e/q_e = 1/b\,q_m + C_e/q_m$$

where q_m is the maximum adsorption capacity corresponding to complete monolayer coverage and b is the equilibrium constant (L/mg). The data fit well to the model with correlation coefficients (R^2) of 0.990, and the maximum adsorption capacity in the studied concentration range is 454.5 mg/g.

The Freundlich model can take the following linearized form:

$$\log q_e = \log k_f + \frac{1}{n_f}\log C_e$$

where K_f is is roughly an indicator of the adsorption capacity and $1/n_f$ is the adsorption intensity. The slope $1/n_f$ ranging between 0 and 1 is a measure of adsorption intensity or surface heterogeneity, becoming more heterogeneous as its value gets closer to zero.[52] The constants are determined by using linear regression analysis and are presented in Table 4. As seen from Table 4, the Freundlich model is not suitable for describing the adsorption equilibrium of dye by functionalized SBA-15 and Langmuir isotherm model yielded the best fit with the highest R^2 value compared to the Freundlich model.

As the results show, the maximum adsorption capacity in the studied concentration range is 454.5 mg/g for AB 214. Three sulphate groups in AB 214 increase the electrostatic attractions between acid dye molecule and fluorene functionalized SBA-15 surface. Therefore, the adsorption capacity of fluorene functionalized SBA-15 for AB 214 seems to be enough high and these adsorbent can be suitable for the large-scale removal of the pollutant dye from wastewater.

Desorption and reuse study

In order to evaluate the possibility of regeneration and reuse of the adsorbent, desorption experiments have been performed. Dye desorption was conducted by washing the dye loaded on fluorene functionalized SBA-15 using ethanol and sodium solution. For this purpose, 5.0 mL of ethanol or 2.0 M sodium hydroxide solution was added to the 5.0 mg of dye loaded adsorbent in a beaker. The concentration of dye in the desorbed solution was measured spectrophoto-metrically. Three cycles of adsorption-desorption studies were accordingly carried out. The results showed desorption efficiencies for sodium hydroxide (96%) was higher than ethanol (85%). It is notable that the equilibrium of desorption was achieved rapidly within about 5 min, similar to the adsorption equilibrium. After the elution of the adsorbed dyes, the adsorbent was washed with DDW and dried under vacuum at 25°C and reused for dyes removal. The reusability of the sorbent was greater than 3 cycles without any loss of sorption capacity Therefore, the fluorene functionalized SBA-15 can be a good reusable and economical sorbent.

Conclusion

A simple and effective method is presented for removal of AB214 from water samples using fluorene functionalized SBA-15. The adsorbent is very effective in removing acidic dye and the adsorption of dyes to functionalized SBA-15 agrees well to the Langmuir adsorption model with maximum adsorption capacities of 454.5 AB 214. The higher adsorption capacity of fluorene functionalized SBA-15 may be explained due to the fact that it proceeds via electrostatic interaction and hydrogen bond formation between the surface of the adsorbent and acid dye. Adsorption kinetics of AB 214 on the prepared adsorbent follow the pseudo-second-order kinetic model. The adsorption of dye to fluorene functionalized SBA-15 is fast and the short duration of this experiment has significant practical importance. Also the preparation of fluorene functionalized SBA-15 is easy and low cost and the process of purifying water pollution is clean and safe. Hence, this methodology can be suitable for the large scale removal of the pollutant dyes from water.

Acknowledgements

The author thanks the Islamic Azad University of savadkooh branch research council for support of this work.

References

1 Swaminathan, K, Pachhade K & Sandhya S, *Desalination*, 186 (2005) 155.
2 Forgacs E & Cserháti T, Oros G, *Environ Int*, 30 (2004) 953.
3 Dos Santos A B, Cervantes F J & Van Lier J B, *Bioresour Technol*, 98 (2007) 2369.
4 Daneshvar N, Khataee A R, Amani Ghadim A R & Rasoulifard M H, *J Hazard Mater*, 148 (2007) 566.
5 Wu C H, Chang C L, *J Hazard Mater B,* 128 (2006) 265.
6 Anjaneyulu Y, Sreedhara Chary N & Samuel Suman Raj D, *Rev Environ Sci Biotechnol*, 4 (2005) 245.
7 Saratale R G, Saratale G D, Chang J S & Govindwar S P, *J Taiwan Inst Chem Eng*, 42 (2011) 138.
8 Wu C H, Kuo C Y & Chang C L, *React. Kinet Catal Lett*, 91 (2007) 161.
9 Golder A K, Hridaya N, Samanta A N & Ray S, *J Hazard Mater B*, 127 (2005)134.
10 Behin J, Farhadian N , Ahmadi M & Parvizi M, *J Water Process Eng*, 8 (2015)171.
11 Chern J M & Huang S N, *Ind Eng Chem Res*, 37 (1998) 253.
12 Capalash N & Sharma P, *World J Microbiol Biotechnol*, 8 (1992) 309.
13 Tripathi P, Chandra Srivastava V & Kumar A, *Desalination*, 249 (2009) 1273.
14 Gadm H M H & El-Sayed A A, *J Hazard Mater*, 168 (2009) 1070.
15 Gupta V K, Mittal A, Kurup L & Mittal J, *J Colloid Interface Sci*, 304 (2006) 52.
16 Ferrero F, *J Environ Sci*, 22 (2010) 467.
17 Li L, Liu S & Zhu T, *J Environ Sci*, 22 (2010) 1273.
18 Mittal A, Gupta V K, Malviya A & Mittal J, *J Hazard Mater*, 151 (2008) 821.
19 Chang S H, Wang K S, Li H C, We M Y & Chou J D, *J Hazard Mater*, 172 (2009) 1131.
20 Zhao K, Zhao G, Li P, Gao J, Lv B & Li D, *Chemosphere,* 80 (2010) 410.
21 Rajeev J, Megha M, Shalini S & Alok M, *J Environ Manage,* 85 (2007) 956.
22 Allen S J G & Mckay Porter J F, *J Colloid Interface Sci,* 280 (2004) 322.
23 Karaca S, Gurses A, Acıkyıldız M & Ejder M, *Microporous Mesoporous Mater,* 115 (2008) 376.
24 Dehghan Abkenar S, Khoobi M, Tarasi R, Hosseini M, Shafiee A & Ganjali M R, *J Environ Eng,* 141 (2015) 1.
25 Alpat K S, Ozbayrak O, Alpat S & Akcay H, *J Hazard Mater,* 151 (2008) 213.
26 Yuan B, Qiu L G, Su H Z, Cao C L & Jiang J H, *Int J Biolog Macromol,* 82 (2016) 355.
27 Ai L, Zhou Y & Jiang J, *Desalination,* 266 (2011) 72.
28 Ho K Y, Mckay G &Yeung K L, *Langmuir,* 19 (2003) 3019.
29 Anbia M, Asl Hariri S & Ashrafizadeh S N, *Appl Surf Sci,* 256 (2010) 3228.
30 Anbia M & Salehi S, *Dyes and Pigments*, 94 (2012)1.
31 Badiei A, Norouzi P & Tousi F, *Europ J Sci Res,* 12 (2005) 39.
32 Badiei A, Bonneviot L, Crowther N & Mohammadi Ziarani G, *J Organomet Chem*, 691 (2006) 5923.
33 Anbia M & Hariri S A, *Desalination*, 261 (2010) 61.
34 Qin Q, Ma J & Liu K, *J Hazard Mater*, 162 (2009) 133.
35 Asouhidou D D, Triantafyllidis K S, Lazaridis N K & Matis K A, *Colloids Surf A, 346* (2009) 83.
36 Zhao D, Feng J, Huo Q, Melosh N, Fredrckson G, Chmelka B & Stucky G D, *Science,* 279 (1998) 548.
37 Badiei A, Goldooz H & Mohammadi Ziarani G, *Appl Surf Sci*, 257 (2011) 4912.
38 Hamoudi S, El-Nemr A & Belkacemi K, *J Colloid Interface Sci*, 343 (2010) 615.
39 Yadavi M, Badiei A, Mohammadi Ziarani G & Abbasi A, *Chem Papers*, 67 (2013) 751.
40 Zhao D Y, Huo Q S, Feng J L, Chmelka B F & Stucky G D, *J Am Chem Soc*, 120 (1998) 6024.
41 Sampay J R & Emmet Reid E, *J Am Chem Soc* 69 (1947) 234.
42 Kruk M, Jaroniec M, Ko C H & Ryoo R, *Chem Mater,* 12 (2000) 1961.
43 Sing K S W, Everett D H, Haul R A W, Moscou L, Pierotti R A, Rouquerol J & Siemieniewska T, *Pure Appl Chem*, 57 (1985) 603.
44 Yadavi M, Badiei A, Ziarani G M & Abbasi A, *Chem papers*, 67 (2013) 751.
45 Socrates G, *Infrared and Raman Characteristic Group Frequencies*, (John Wily) 2004.
46 Yadavi M, Badiei A & Ziarani G M, *Appli Surf Sci*, 279 (2013) 121.
47 Jaroniec C P, Kruk M, Jaroniec M & Sayari A, *J Phys Chem B*, 102 (1998) 5503.
48 Lagergren S, *Handlingar*, 24 (1898) 1.
49 Ho Y S & McKay G, *Chem Eng J*, 70 (1998) 115.
50 Langmuir I, *JACS,* 38 (1916) 2221.
51 Freundlich H M F, *J Phys Chem*, 57 (1906) 385.
52 Haghseresht F & Lu G, *Energy Fuels*, 12 (1998) 1100.